Sarap Krishnaprasad[1,2], Mohammed Shareefuddin[1], Siddey Laxmi Srinivasa Rao[3], Gokarakonda Ramadevudu[41]*

[1]Department of Physics, Osmania University, Telangana, Hyderabad, India; [2]SRR Government Arts & Science College (A), Karimnagar, Telangana, India; [3]Department of Physics, Government City College (A), Hyderabad; [4]Department of Physics, Vasavi College of Engineering (A), Telangana, Hyderabad, India

Scientific Paper
ISSN 0351-9465, E-ISSN 2466-2585
https://doi.org/10.62638/ZasMat1147

Zastita Materijala 65 (4)
561 – 577 (2024)

Structural Investigation and Physical Properties of RO-ZnO-$Li_2B_4O_7$-$K_2B_4O_7$ (RO= SrO and BaO) Glasses

ABSTRACT

Glass samples 10RO-30ZnO-x$Li_2B_4O_7$-(60-x) $K_2B_4O_7$ (RO=SrO and BaO) with alkali tetra borates varying from 0 to 60 mol% were produced by traditional quenching procedure. Peak free broad X-ray diffraction patterns established the amorphous feature of glass samples. FTIR and Raman spectroscopic analysis showed the existence of BO_3 and BO_4 structural groups and other borate units. The $BO_3 \Leftrightarrow BO_4$ conversion rate was not much affected by variation in one of the alkali-tetrabo-rates. EPR spectra of copper doped glasses confirmed the ground state of Cu^{2+} ions as $^2B_{1g}$. Physical and optical properties namely density, molar volume, refractive index, molar refractivity, optical band gap and Urbach energy values were found to be composition dependent. The inflections observed in density, and other optical properties around equal mol.% of alkali oxides in the glass system were attributed to structural modifications and mixed alkali effect. These results exposed the structural variations caused by competitiveness between the two different alkali and alkaline oxides in occupying the geometrical positions of the borate glass network.

Keywords: *mixed alkali effect (MAE), alkaline earth-oxide glasses, optical bandgap, electron paramagnetic resonance, FTIR and Raman spectroscopy*

1. INTRODUCTION

Mixed alkali and alkaline earth oxide borate glasses containing various dopants got popularity due to their utilization in various sectors including solid state ionics, bio-active glasses, host materials for lasers, radiation shielding, memory applications, electronic devices, acoustics, solar cells, energy storage, sensors, laser, and infrared detection etc. [1-6]. The oxides Li_2O, Na_2O, K_2O, MgO, CaO, SrO, BaO, ZnO, PbO etc., are extensively used as glass modifiers or additional formers (depending on their mol%) added in conjunction with B_2O_3. The glass modifiers are used to improve the physical, electrical, mechanical, and optical properties of oxide glasses. Borate glasses consisting of different alkali and alkaline earth oxides can be prepared below 1200°C temperature with ease by quenching.

Addition of ZnO into borate glass network particularly improves optical properties and stability. The role of ZnO changes from glass modifier to glass former if its composition is greater than 45 mol % [7]. The alkaline earth oxides SrO and BaO in general extend the glass producing ability as network modifiers or formers depending on their mol% in the glass matrix. These two oxides improve the chemical durability of the glass. It was reported by researchers that these oxides act as glass modifiers at low concentration (below 30%) and formers when their content is high [8-10].

Borate glasses with rich alkali content display boron anomaly namely “Mixed Alkali Effect” (MAE) when two or more than two alkali oxides are present in the glass matrix. Similarly mixed alkaline oxides also exhibit a similar phenomenon namely “Mixed Alkaline Effect”. The MAE induces significant

* Corresponding author: Gokarakonda Ramadevudu
E-mail: dr.ramdev@gmail.com
Paper received: 31.1.2024.
Paper accepted: 11.04.2024.

changes in many physical, electrical, and optical properties of glasses when one alkali/ alkaline oxide is replaced by the other alkali/alkaline oxide. The observed changes might result in due to the competitive role of occupation of different structural positions by the alkali/alkaline oxide ions. The varying content of alkali oxides favours sudden or gradual changes in various properties and exhibits positive or negative inflections around equal mole percentage of the two alkali oxides in the glass composition [11-13].

The mixed effect of glass formers or glass modifiers such as SrO and BaO results in significant variation of glass properties, in addition to effect the glass formation. It was observed that presence of two glass modifier oxides SrO and BaO reduces the diffusion because of the competition between them. The heavy oxide BaO in general disrupts the glass network by forming non-bridging oxygens (NBO) and thereby causes change in structure as well as physical and optical properties [14-16]. Glasses containing mixed alkaline oxides show interesting properties such as increased thermal stability and decreasing mechanical properties. Ternary borate glasses containing SrO have shown improved bioactivity [17,18].

There are a few studies on structural and physical properties in the literature on glasses containing double tetraborates. The studies on the role of alkaline oxides in tetraborate glasses scarcely found. The present work investigates the effect of alkali tetraborate oxides on the structural units of the glass, spectroscopic parameters, physical and optical properties of 10RO-30ZnO-x$Li_2B_4O_7$-(60-x) $K_2B_4O_7$ (RO=SrO and BaO) glass system. This paper analyzes the role of RO and ZnO as glass modifiers. The role played by alkali ions in occupying various structural locations was also discussed. In the base glass, copper oxide (CuO) is added to undertake electron paramangetic resonance studies and to know the nature of lignad field in the surroundings of the spin probe Cu^{2+} ion. By estimating Hamiltonian parameters and the bonding coefficients the ground state of Cu^{2+} ion is determined.

2. EXPERIMENTAL TECHNIQUES

10RO-30ZnO-x$Li_2B_4O_7$-(60-x)$K_2B_4O_7$ (RO=SrO, BaO) were made by quenching process. The present glass compisition contained ZnO at fixed 30 mol% and alkaline earth oxide content retained constant at 10 mol%. The alkali tetraborate oxides were gradually swapped in the glass matrix from 0 to 60 mol%. The base glass composition was doped with 1 mol% of CuO to make fresh glasses 10RO-30ZnO-x$Li_2B_4O_7$-(59-x)$K_2B_4O_7$-1CuO (RO=SrO, BaO) for EPR and optical absorption analysis. $Li_2B_4O_7$ (Sigma-Aldrich), $K_2B_4O_7$ (Sigma-Aldrich), SrO (Sigma-Aldrich), BaO (Sigma-Aldrich), ZnO (SDfine), and CuO (SDfine) were the starting chemical ingredients in mol%. These chemicals were mixed throughly in approriate amounts in a mortor and pestle. Then the mixtures taken in porcelain crucibles were melted at around 1100^{0}C temperature for half-an-hour.

The uniform and homogenious vitreous melts were instantly poured onto a stainless steel plate held around 200^{0}C. The melts were immediately flattened with another steel plate. The prepared glass samples were annealed at 200^{0}C for nearly 2 hour to relieve the leftover internal mechanical stresses and brought them to room temperature gradually. In the present study, the annealing temperature was chosen from the literature corresponding to alkali-alkaline borate glasses and accordingly annealing was done at 200^{0}C. The glasses thus made were very clear, transparent and prepared in disc and rod shapes for characterization.

The X-ray patterns were taken on Bruker D8 Advance machine. The optical measurements were carried on samples of average thickness 0.5mm. Smaller the thickness of the sample better will be the approximation in the optical bandgap energy measurements. The optical absorption spectra were scanned on Agilent technologies-Carry 5000 with UMA spectrophotometer (wavelength range 200-1100 nm). FTIR spectra were recorded on SHIMADZU–8400S spectrometer (wavenumber range 400–4000cm^{-1}). LAB RAM HR Horiba France with 532 nm Nd-YAG laser 100 mW Raman Spectrometer was used to get Raman spectra (wavenumber range 200–2000 cm^{-1}). The electron paramagnetic resonance spectra of Cu^{2+} ions were recorded on JES - FA200 ESR Spectrometer in X-band (8.75-9.65 GHz) frequencies keeping the a field modulation of 100 KHz. The magnetic field was varied between 250mT and 400 mT. All the above measurement were made at room temperature. The refractive index values of the glass samples were determined from the optical bandgap (E_{opt}) values. The glass codes and compositions of the prepared glass samples were given in **Table.1.**

3. RESUTLS AND DISCUSSION

3.1. X-ray diffraction

Fig.1 represents x-ray diffraction shapes of 10RO-30ZnO-x$Li_2B_4O_7$-(60-x) $K_2B_4O_7$ (RO= SrO, BaO) glasses. The broad x-ray diffractograms with no sharp peaks indicated amorphous nature of the present glass samples.

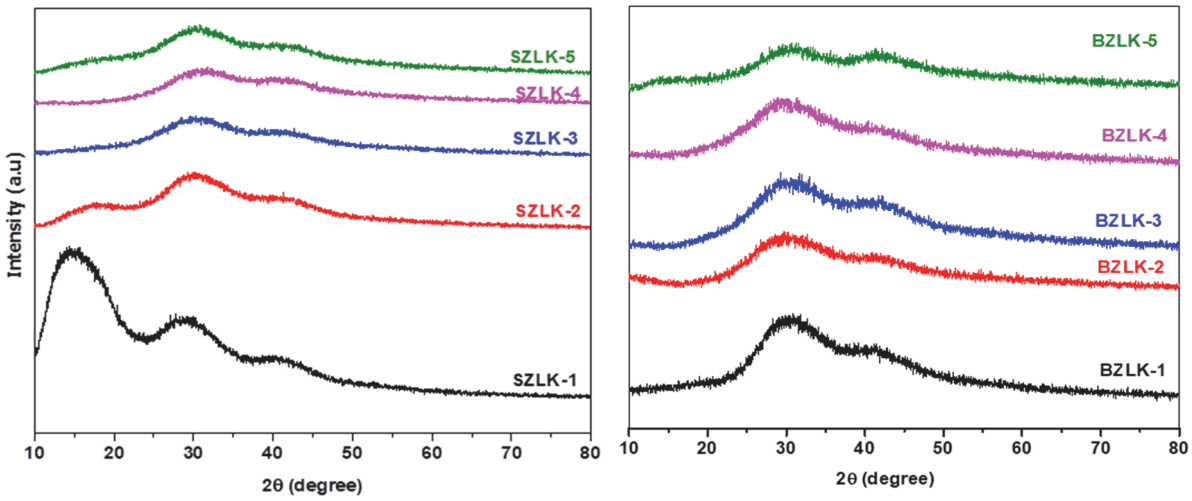

Figure 1. X-ray diffraction patterns of 10RO-30ZnO-x$Li_2B_4O_7$-(60-x)$K_2B_4O_7$ (RO= SrO and BaO) glasses

3.2. Structural characterization

3.2.1. Fourier Transform Infrared (FTIR) studies:

Fig.2 illustrates Fourier Transform Infrared (FTIR) spectra of SZLK1 to SZLK5 and BZLK1 to BZLK5 glasses. The characteristics fingerprint peak positions (400 to 1600 cm^{-1}) of borate glasses are clearly visible in **Fig.2**. It is well established fact that the infrared active bands of several borate glasses appear in three categories specifying bending vibrations between 600cm^{-1} and 800cm^{-1}, stretching vibrations of BO_4 units (800-1200 cm^{-1}) and BO_3 units (1200 –1600 cm^{-1}) stretching vibrations. The band position between 2200 to 4000 cm^{-1} corresponds to H-O-H and OH^- groups vibrations. These three primary vibrations are detected in the FTIR spectra of the glass samples. In addition to the borate vibrational bands, there are bands about 440 cm^{-1} due to the presence of cations like Zn^{2+} ions.

Various infrared peaks observed between 400 to 4000 cm^{-1} and their assignments are provided in **Table.2**. From **Fig.2** it is apparent that both SZLK and BZLK glasses contained similar IR bands with a slight shift in wave numbers. The observed shifts are as expected due to the difference in the molar masses of SrO (103.62 g/mol) and BaO (153.33 g/mol). The IR bands at lower wave numbers between 440 and 480cm^{-1} in SZLK and BZLK glasses respectively correspond to existence of Zn^{2+} metal cations and Zn-O bond vibration from ZnO_4 tetrahedral units [19,20]. These vibrational frequencies indicated formation of Zn-O bonds in the glass network. The structures also contain Sr^{2+} cations in SZLK glasses and Ba^{2+} cations in BZLK glass matrix.

Table.1 Composition and codes of 10RO-30ZnO-x$Li_2B_4O_7$-(60-x) $K_2B_4O_7$ Glass Systems

Glass code	pure samples (SZLK/BZLK) (mol%)				
	SrO	BaO	ZnO	$Li_2B_4O_7$	$K_2B_4O_7$
SZLK1	10	-	30	0	60
SZLK2	10	-	30	15	45
SZLK3	10	-	30	30	30
SZLK4	10	-	30	45	15
SZLK5	10	-	30	60	0
BZLK1	-	10	30	0	60
BZLK2	-	10	30	15	45
BZLK3	-	10	30	30	30
BZLK4	-	10	30	45	15
BZLK5	-	10	30	60	0

Various infrared peaks observed between 200 to 4000 cm^{-1} and their assignments are provided in **Table.2**. From **Fig.2** it is apparent that both SZLK and BZLK glasses contained similar IR bands with a slight shift in wave numbers. The IR bands at lower wave numbers between 440 and 480cm^{-1} in SZLK and BZLK glasses respectively correspond to existence of Zn^{2+} metal cations and Zn-O bond vibration from ZnO_4 tetrahedral units. These vibrational frequencies indicated formation of Zn-O bonds in the glass network.

The characteristic boroxol ring vibrations (806 cm^{-1}) [21] are absent in the present glass samples. Infrared peaks of small intensity detected in the range 600-800 cm^{-1} are attributed to bending of B-O linkages. The bands occurring in 900-1200 cm^{-1} region are arising from asymmetric stretching vibration of BO_4 units. Peaks around 1230–1630 cm^{-1} are assigned to stretching of BO_3^- units belonging to meta, pyro and ortho borate networks. Ali and Rammah et al also observed borate group vibrations in the range 800-1200 cm^{-1} and attributed them to stretching vibrations of B-O units present in BO_4 groups [22]. The concentration of BO_3 (i.e. N_3) and BO_4 (i.e. N_4) units is found to vary in a non-linear manner with $Li_2B_4O_7$ composition. Therefore, exchange of bridging oxygens to non-bringing oxygens or $BO_3 \Leftrightarrow BO_4$ transformation with $Li_2B_4O_7$ mole % in the glass matrix can be assumed to be trivial. Accordingly, the present glasses contain a complex structure having blend of (BO_3), (BO_4) with bridging and non-bridging oxygens, >B–O– end groups and zinc-borate groups. Although Zinc oxide may not have played major role in the transformation of BO_3 units into BO_4 units but efficient to form zinc-borate complexes such as ZnO_4 [10, 23].

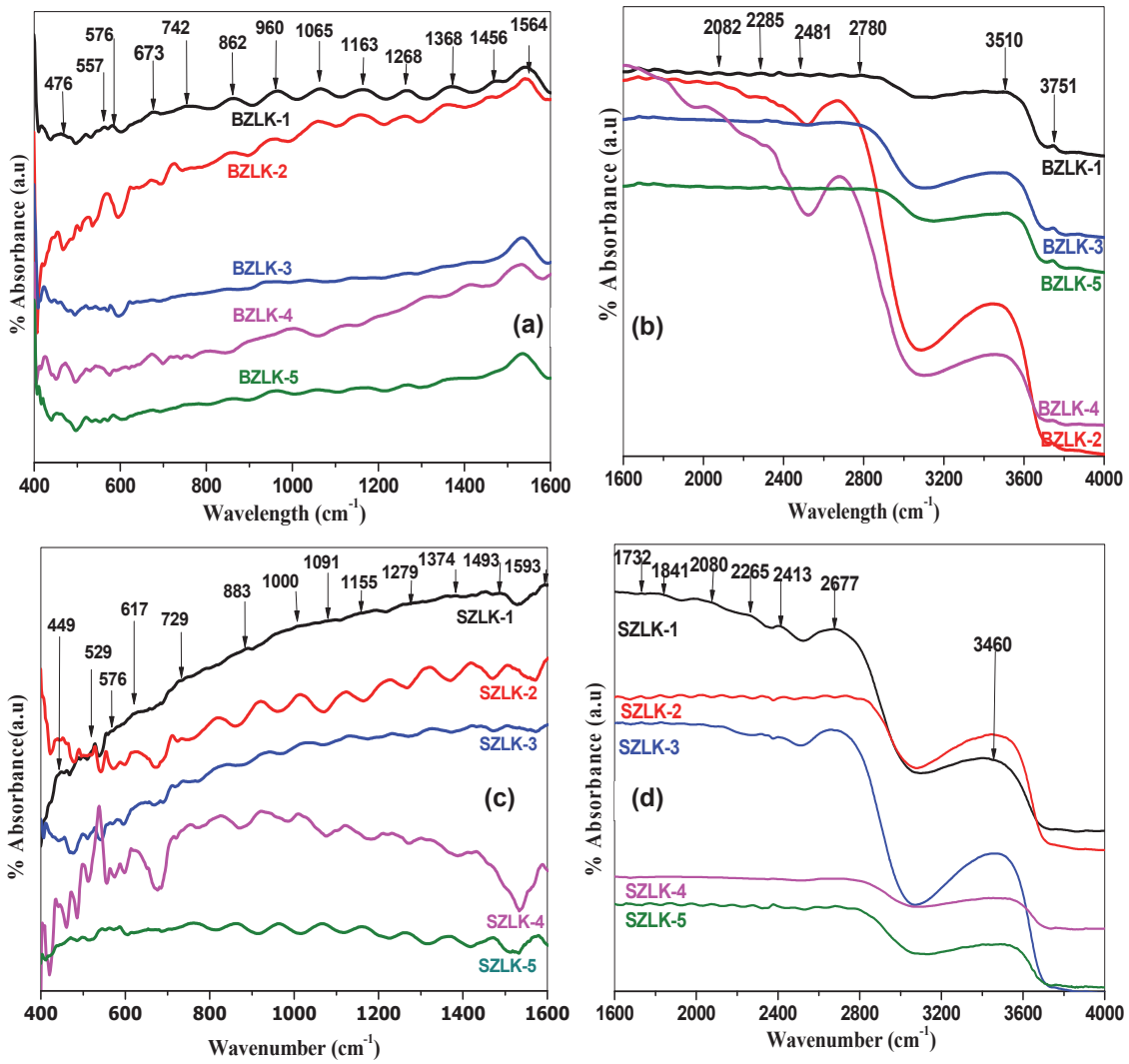

Figure 2. FTIR spectra: a) BZLK 400-1600 cm^{-1} b) BZLK 1600-4000 cm^{-1} c) SZLK 400-1600 cm^{-1} and d) SZLK 1600-4000cm^{-1}.

It can be concluded from FTIR studies that both SZLK and BZLK glasses did not exhibit vibrational peak at 806 cm^{-1} corresponding to boroxol rings in their glass structure [21]. Zinc oxide and alkaline earth oxides could have gradually converted boroxol rings into diborate, triborate, tetra and penta borate units of BO_3 and BO_4 groups. Ultimately the present glass structural landscape consists of BO_3 and BO_4 groups which in turn are interconnected in the random glass network. These structural units are not uniformly distributed and randomized with progressive substitution of $Li_2B_4O_7$ [23,24]. In addition, metal cations Li^+ and K^+ vibrations are also observed due to the presence of infrared peaks between 530 and 560 cm^{-1} [25].

3.2.2. Raman Spectroscopic studies

Fig.3 depicts Raman spectra of SZLK and BZLK glasses. The Raman bands involved are clearly identified by using deconvolution spectra. Some of the Raman peaks are not resolved clearly. For better identification of Raman peak locations deconvolution spectra is used. The deconvoluted spectra of SZLK-1 and BZLK-1 are given in **Fig.4**. A similar approach of deconvolution is used for the other samples of the present study. Raman band assignments are presented in **Table.3**.

Table.2 FTIR band assignments of SZLK and BZLK glass samples

FTIR peak positions Wavenumber (cm^{-1})					Band Assignments
SZLK1	**SZLK2**	**SZLK3**	**SZLK4**	**SZLK5**	
449	443	449	443	462	Zn^{2+} metal cation vibrations and Zn-O bonds vibrations from ZnO_4 tetrahedral [19,20]
529	531	533	538	542	Li^+ and K^+ metal cations vibrations [25]
576	588	588	588	590	Sr-O vibrations and Zn-O bending vibrations [26]
617-737	636-724	649-737	600-718	649-774	B-O-B bending vibrations in BO_3 units [26,27]
883-1155	919-1211	926-1155	921-1180	965-1155	B—O stretching vibrations of tri, tetra, penta and diborate units of BO_4 groups [26]
1279-1593	1227-1636	1230-1630	1230-1593	1268-1580	B-O asymmetric stretching vibrations of [BO_3] trigonal units in meta-, pyro-and orthoborate units [26]
		2200–3000			H–O–H bending vibrations (hydrogen bonds) [27]
		3200–3600			Hydroxyl/ water groups stretching vibration [27]
BZLK1	**BZLK2**	**BZLK3**	**BZLK4**	**BZLK5**	
476	483	470	483	456	Zn^{2+} metal cation vibrations and Zn-O bonds vibrations from ZnO_4 tetrahedral units [19,20]
551	560	549	551	553	Li^+ and K^+ metal cations vibrations [25]
576	569	572	576	581	Ba-O vibrations and Zn-O bending vibrations [26]
673-862	667-854	667-854	673-824	660-856	B-O-B bending vibrations in BO_3 units [26,27]
960-1163	966-1161	945-1170	980-1194	987-1177	B—O stretching vibrations of tri, tetra, penta and diborate units of BO_4 groups [26]
1272-1564	1265-1564	1299-1545	1286-1537	1380-1681	B-O asymmetric stretching vibrations of [BO_3] trigonal units in meta-, pyro-and orthoborate units [26]
		2200–3000			H–O–H bending vibrations (hydrogen bonds) [27]
		3200–3600			Hydroxyl/water groups stretching vibration [27]

From the Raman and FTIR spectroscopic analysis the structural groups present in the glass samples are diborate, triborate, tetra and penta borate units of BO_3 and BO_4 groups. The structure has meta borates and pyroborate groupings. Eventually the structure of both SZLK and BZLK consists of interconnected random glass network of several structural units [33-37].

Both the glass systems under investigation have shown Raman bands almost at the same peak positions with slight shift. From the deconvolution spectra, it is inferred that with varying $Li_2B_4O_7$ mole %, the Raman band intensities varied non-uniformly. The observed non-linear changes can be assigned to mixed alkali effect. Similar results also had been reported by Padmaja et al. [26,27].

Fong et al attributed bands below 300 cm^{-1} to metal ion vibrations [28]. Existence of Sr^{2+} and Ba^{2+} ions respectively in SZLK and BZLK glasses and Zn-O stretching and bending vibrations of O-Zn-O of ZnO_4 tetrahedra are noted from the Raman bands around 277 cm^{-1}. Raman Peaks and shoulders around 430-500 cm^{-1} corresponds to diborate groups vibrating in isolation and such Raman bands were also reported by Anghel et al [29]. The bands in the range 679 to 774 cm^{-1} corresponds to six-membered borate rings breathing vibrations of BO_3 and BO_4 unis. A high intense peak around 770cm^{-1} depicts the existence of symmetric breathing vibration of six-membered rings with one BO_4 tetrahedron i.e., triborate, tetraborate or penta-borate units. Maniu et al also seen strong band at ~770 cm^{-1} in potassium borate glasses holding TiO_2 [30]. Raman bands that appeared at wavenumbers 940 and ~1070 cm^{-1} proved the formation and existence of metaborates induced in the network due to alkaline earth oxides SrO/BaO. Tetsuji Yano et al ascribed Raman bands in the range 1100- 1600cm^{-1} to vibration modes of BO_2O– triangles connected with other borate triangular units and short-range structures of BO_3 [31]. The broad region of bands between 1320–1600 cm^{-1} are associated with B-O^- bond stretching vibrations connected with triangular borate units [32]. The intensity of vibrational bands corresponding to [BO_4] units slightly decreased while intensity of [BO_3] bands slightly increased and broadened, but substantial change in the intensity of the peaks is not seen.

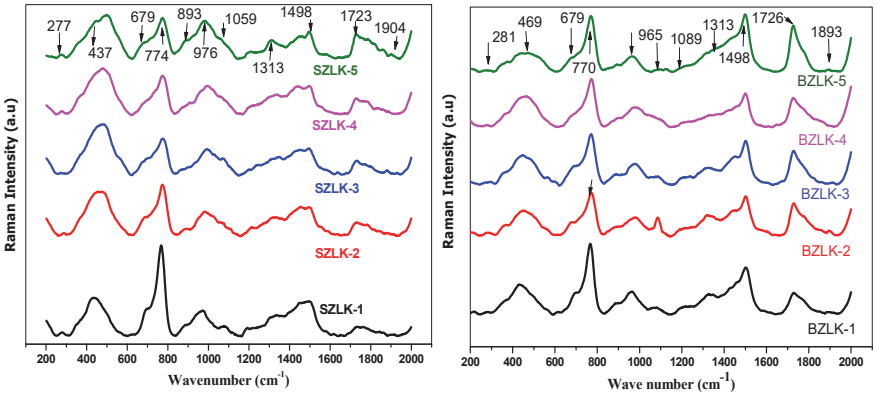

Figure 3. Raman spectra of 10RO-30ZnO-x$Li_2B_4O_7$-(60-x)$K_2B_4O_7$ (RO= SrO and BaO) glass systems

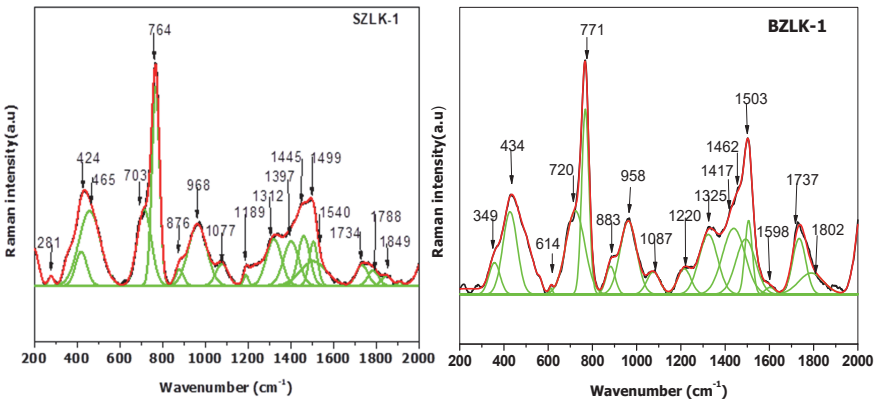

Figure 4. Deconvoluted Raman spectra of SZLK-1 and BZLK-1 glass systems

Table.3 Raman band assignments of SZLK and BZLK glass samples

Raman bands Wavenumber (cm^{-1})					*Band Assignments*
SZLK1	**SZLK2**	**SZLK3**	**SZLK4**	**SZLK5**	
277	288	277	274	277	vibrations of Sr^{2+} ions. Zn-O stretching vibrations and bending vibrations of O-Zn-O of ZnO_4 tetrahedra [28]
498	480	476	473	437	Vibrations of ring angle bending (B–O–B) of borate units or isolated diborate units [29,30]
701	690	694	683	679	bending modes of metaborate chains [20,37].
766	777	777	777	774	Symmetric breathing vibration of six-membered rings with BO_4 tetrahedron i.e., tri-, tetra- or penta borate units [30]
973	984	991	994	976	asymmetric stretching modes of tetrahedral borate BO_4 groups [32,33]
1081	1071	1071	1059	1059	
1321	1335	1342	1335	1313	Stretching vibrations of B–O bonds of large number of borate groups [27, 31]
1498	1502	1498	1502	1498	B-O^-bond stretching vibrations and vibrations of BO_2O^- triangles connected with other borate triangular units and vibration modes of short-range structures of BO_3 [31]
1740	1733	1730	1730	1723	BO stretching vibrations in BO_3 triangular units [27]
1853	1850	1882	1889	1904	
BZLK1	**BZLK2**	**BZLK3**	**BZLK4**	**BZLK5**	
277	284	288	277	281	vibrations of Ba^{2+} ions. Zn-O stretching vibrations and bending vibrations of O-Zn-O of ZnO4 tetrahedra [28]
434	444	451	448	485	Vibrations of ring angle bending (B–O–B) of borate units or isolated diborate units [29,30]
694	679	694	686	679	bending modes of metaborate chains [20,37].
774	774	770	774	770	Symmetric breathing vibration of six-membered rings with BO_4 tetrahedron i.e., tri, tetra or penta borate units [30].
965	980	980	980	965	asymmetric stretching modes of tetrahedral borate BO_4 groups [32, 33].
1078	1092	1089	1103	1089	
1324	1321	1321	1321	1313	Stretching vibrations of B–O bonds of large number of borate groups [27, 31]
1502	1502	1502	1502	1498	B-O^-bond stretching vibrations and vibrations of BO_2O^- triangles connected with other borate triangular units and vibration modes of short-range structures of BO_3 [31]
1730	1730	1730	1726	1726	BO stretching vibrations in BO_3 triangular units [27]
1893	1900	1911	1867	1893	

3.2.3. EPR and Optical absorption of Cu^{2+} ions:

Fresh glass sample-s of 10RO-30ZnO-x$Li_2B_4O_7$–(59-x)$K_2B_4O_7$-1CuO made (SZLKC and BZLKC glasses) to investigate EPR splittings. EPR spectra of Cu^{2+} ion in the SZLK and BZLK glasses are given in **Fig.5** and **Fig.6** depicts Cu^{2+} ion optical absorption spectra of SZLKC and BZLKC glass samples. The errors in the evaluation of g and A values respectively are about ±0.001 and ±2x10^{-4} cm^{-1}.

In general, EPR spectrum of Cu^{2+} ion consists of four parallel and four perpendicular hyperfine components. But only three parallel components in the low magnetic field side are clearly observed. The perpendicular components are not resolved. Similar observations have been reported by several authors [38,39]. Here the fourth parallel component is supposed to overlap with perpendicular components. The EPR spectrum was analyzed with the help of axial spin Hamiltonian [39]:

$$\mathcal{H} = \beta[g_{\parallel}H_Z S_Z + g_{\perp}(H_X S_X + H_Y S_Y)] + A_{\parallel} I_Z S_Z + A_{\perp}(I_X S_X + I_Y S_Y) \quad (1)$$

The parallel ($g_{//}$) and perpendicular ($g_{\perp}$) components of *g*-tensor and parallel ($A_{//}$) and perpendicular ($\mathbf{A}_{\perp}$) components of *A*-tensor are obtained from the EPR spectra of present glasses doped with the Cu^{2+} ions. The optical absorption maxima of Cu^{2+} are designated to the $^2B_{1g} \rightarrow {}^2B_{2g}$ transition. The spin-Hamiltonian, bond parameters and covalency values are listed in **Table.4**. The various parameters are evaluated using the equations given below with different terms having usual meanings [40,41].

$$h\nu = g_{ll}\beta H + mA_{ll} + \left(\frac{15}{4} - m^2\right)\frac{A_{\perp}^2}{2\beta H g_{ll}} \quad (2)$$

$$h\nu = g_{\perp}\beta H + mA_{\perp} + \left(\frac{15}{4} - m^2\right)\frac{A_{\perp}^2 + A_{ll}^2}{4\beta H g_{ll}} \quad (3)$$

$$\Delta E_{xy,yz} = \frac{1656K^2}{g_{\perp} - 2.0023} \quad (4)$$

$$\alpha^2 = -\left(\frac{A_{ll}}{P}\right) + (g_{ll} - 2) + \frac{3}{7}(g_{\perp} - 2) + 0.04 \quad (5)$$

$$\beta^2 = \left(\frac{g_{\perp}}{g_e} - 1\right)\frac{\Delta E_{xy,yz}}{828\alpha^2} \quad (6)$$

$$\beta_1^2 = \left(\frac{g_{ll}}{g_e} - 1\right)\frac{\Delta E_{xy}}{3312\alpha^2} \quad (7)$$

$$\tau_{\sigma} = \frac{200(1-S)(1-\alpha^2)}{1-2S}\% \quad (8)$$

$$\tau_{\pi} = 200(1 - \beta_1^2)\% \quad (9)$$

Here *S* is the overlap integral and S_{oxy} has a value of 0.076.

The estimated $g_{//}$ values of present glasses are noted to be higher than $g_{\perp}$ values and $A_{//}$ values are larger than $A_{\perp}$ values. This type of conduct reveals Cu^{2+} ions inhabiting in stretched octahedral sites ($g_{//} > g_{\perp} > g_e$=2.0023) in the glass. The ground state of Cu^{2+} ion is attributed to $d_{x^2-y^2}$. From the EPR spectra, it is observed that peak intensity in SZLKC glass samples increased from SZLKC1 to SZLKC5 indicating a greater number of Cu^{2+} ions participating in the resonance. In BZLKC glass system peak intensity increased from BZLKC1 to BZLKC4, while BZLKC5 peak intensity decreased indicating non-linear variation of Cu^{2+} ion concentration in the glass samples.

Fig.7 reveals that $g_{//}$ and $A_{//}$ values varied non-linearly with $Li_2B_4O_7$ mole %. Many alkali/alkaline earth oxide containing borate glasses display such type of behaviour [25,32,38]. When an alkali tetra borate ($K_2B_4O_7$) is substituted by another alkali tetra borate ($Li_2B_4O_7$) in the glass composition, there occurs a race between the two alkali ions in occupying sites in the glass network and hence the variation of $g_{\parallel}$ and $A_{\parallel}$ is non-linear which can be attributed to mixed alkali effect (MAE) which cuased due to strutural adjustments. The mixed alkali effect is known for improving glass properties and its applications in various areas including bioactive glasses [42].

The bonding coefficients α^2, β^2, and β_1^2 respectivey corresponds to in-plane σ- and π- bondings and out-of-plane π bonding of Cu(II) complex. These values (**Table.4**) are close to unity. Hence the bonding coefficients signifies moderate ionic charcter of the galsses under study.

The incorporation of copper ions into the glass matrix breaks down some of B-O-B bonds and thereby responsinble for formation of other borate structural units such as creation of Non-Bridging Oxygens (NBOs) or conversion of BO_3 units into BO_4 units occurs. However, in the present glass system no significant structural changes are observed due to doping of copper as the mole percent of CuO is kept constant at a low value of 1 mol%.

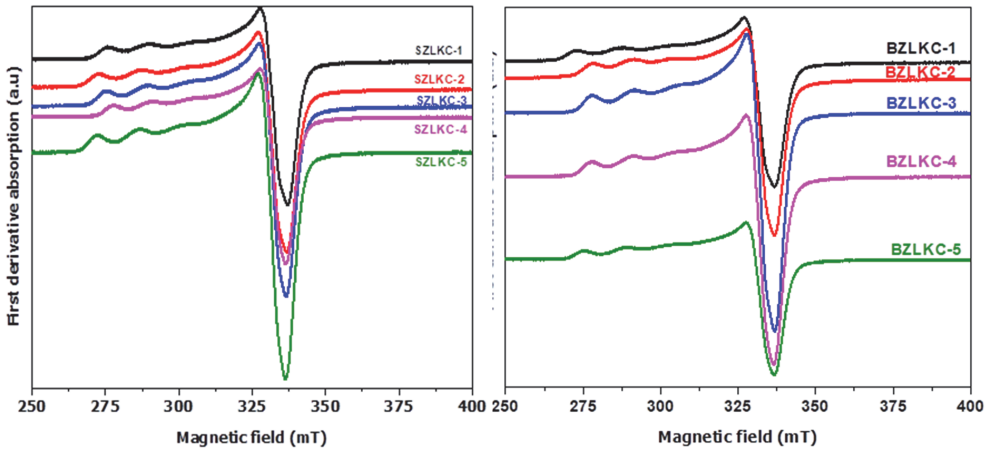

Figure 5. EPR spectra of copper ions in SZLKC and BZLKC glass systems

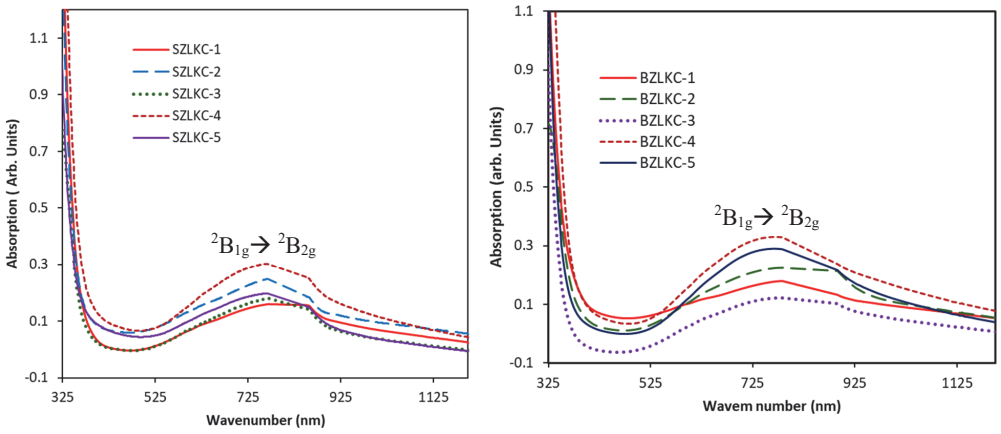

Figure 6. Optical absorption spectra of SZLK and BZLK glass systems

Table.4 EPR Parameters of SZLKC and BZLKC glass samples

Glass Code	$g_{\parallel}$	$g_{\perp}$	$A_{\parallel} x10^{-4}$ (cm^{-1})	$A_{\perp} x10^{-4}$ (cm^{-1})	ΔE_{xy} (cm^{-1})	$\Delta E_{xy,\,yz}$ (cm^{-1})	α^2	β^2	β_1^2	τ_σ %	τ_π %
SZLKC1	2.284	2.036	138	31	12630	29134	0.722	0.820	0.741	60.58	51.80
SZLKC2	2.297	2.039	147	33	12640	26716	0.762	0.777	0.737	51.87	52.60
SZLKC3	2.284	2.038	141	30	12630	27477	0.732	0.809	0.732	58.40	53.60
SZLKC4	2.271	2.038	135	29	12890	27395	0.703	0.843	0.744	64.72	51.20
SZLKC5	2.302	2.041	147	32	12920	25973	0.767	0.772	0.76	50.78	48.00
BZLKC1	2.299	2.039	144	33	12706	26814	0.756	0.783	0.753	53.17	49.40
BZLKC2	2.266	2.037	138	30	12787	28476	0.707	0.838	0.719	63.85	56.20
BZLKC3	2.376	2.036	138	30	12987	28890	0.815	0.727	0.898	40.32	20.40
BZLKC4	2.276	2.038	130	30	13037	27099	0.693	0.854	0.775	66.90	45.00
BZLKC5	2.289	2.038	135	29	12953	27481	0.720	0.822	0.777	61.02	44.60

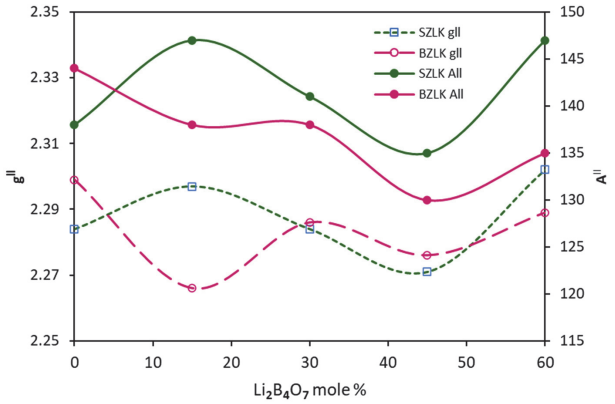

Figure 7. Variaton of g_{II} and A_{II} values with $Li_2B_4O_7$ mol% in SZLKC and BZLKC glass systems

4. PHYISCAL AND OPTICAL PROPERTIES

4.1. Density and Molar Volume:

Using Archimedes liquid immersion process the densities (ρ) of glass samples are measured at room tempertature with Xylene (ρ = 0.86 g/cm^3) as immersion liquid. Three iterations were performed to calculate the density of every sample using the formula [43].

$$\rho = \left(\frac{A}{A-B}\right) * \rho_{xylene} \quad (10)$$

Here A and B are respectively weight of the sample in in xylene and in air. The error in the estimation of density is around ±0.01 g/cc. From the density values molar volume (V_m) of the glass samples are computed by the below given formula with usual notation [43],

$$V_m = \frac{\sum x_i M_i}{\rho} \text{ cm}^3\text{/mol} \quad (11)$$

The density and molar volume values are recorded in **Table.5**. The changes of densities and molar volumes with $Li_2B_4O_7$ mole % are shown in **Fig.8**.

As expected like many other alkali and alkaline earth borate glasses, the present glass samples also have shown opposing trend [39,43]. The density and molar volume normally offer informatiom on the strucuture units since these parameters are closely depend on distribution of fundamental structural units that makes the glass network.

SZLK glasses have low density values compared to BZLK glasses. The molar volume values of SZLK glasses are higher than that of BZLK glasses. It is observed that both densities and molar volumes within each glass series varied in a non-linear maner. The density values increased with increasing content of $Li_2B_4O_7$ (x mol%) in the glass network and except showing a minimum value when $Li_2B_4O_7$ mol% equals to $K_2B_4O_7$ 30 mole % in the glass composition. The higher densities of BZLK systems compared to SZLK glasses are due to high molecular weight of BaO compared to SrO. The molar volume of SZLK and BZLK samples almost decreased linearly with $Li_2B_4O_7$ mol% in the glass matrix showing an inflection at 30 mol%.

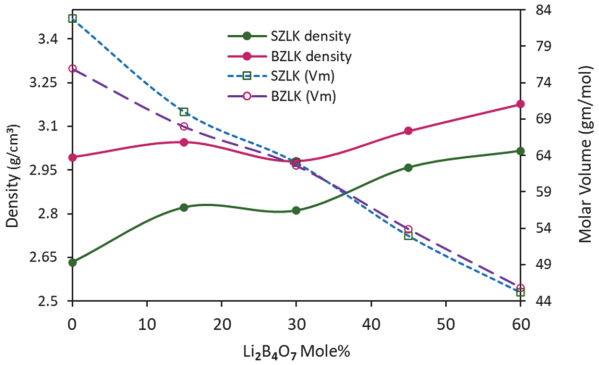

Figure 8. Variation of density and molar volume with $Li_2B_4O_7$ mol%.

The non-linear changes might be assigned to the ionic sizes of the alkali and alkaline ions. The sizes of Li^+ ion (0.076nm), K^+(0.138 nm), Mg^{2+}(0.072nm), Zn^{2+}(0.060nm four coordinated) ions indicate that smaller metal ions like Mg^{2+} and Zn^{2+} might have taken interstitial or void locations. Hence there is competition between ions present in the glass network to occupy various structural locations. Therefore the changes in density and molar volumes could be atttributed to ionic sizes that might have caused the so called mixed alkali effect (MAE) in particular or mixed oxide effect (MOE) in general.

4.2. Optical band gap and Urbach Energy

The power law region is clearly shown in optical absorption spectra. The optical absorption followed Beer-Lambert- Bouguer law. The absorption coefficient α(ω) of a glass sample having thickness 't' is arrived from the expression [44]. According to Tauc, Mott and Davis power law, amorphous materials like glasses obey Tauc's rule [44]

$$\propto(\omega) = \frac{A}{\hbar\omega}.(\hbar\omega - E_{opt})^r \quad (12)$$

Here 'A' is a constant, hω is the incident optical energy, 'r' can have ⅓, ½, 2, 3 values that represents respectivly direct forbidden, direct allowed,

indirect allowed, indirect forbidden transitions. Using above relation the optical energy band gap E_{opt} is evaluated. For the present glass systems the best fit is achieved when r =2. The Tauc plot drawn between (αhν)½ and (*hν*) and are shown in **Fig.9**. If the fundamental absorption energy (*ω*) edge is in low energy range (10^2 to10^4 cm^{-1}), then α(ω) follows Urbach law [44]:

$$\propto(\omega) = B.e^{(\hbar\omega/\Delta E)} \quad (13)$$

where B is a constant and *ΔE* is the Urbach's energy. *ΔE* values are obtained from slopes of the linear portions of the graph shown in **Fig.9**. Urbach energies are estimated from **Fig.10**. The arrived values of optical band gap energies (E_{opt}) and and Urbach energy (*ΔE*) are reported in **Table.5**

The calcluated values E_{opt} and *ΔE* of SZLK and BZLK glasses are in comparison with similar glasses reported in the literature [43-46]. The errors in the calcuation of E_{opt} and *ΔE* respectively about ±0.05 eV and ±0.005eV. E_{opt} and Urbach energies have shown varied differently with $Li_2B_4O_7$ mol% in the glass (**Fig.11**). Optical band gap energies and Urbach have shown a marked change when the two alkali tetraborates are equal.

Glasses show static and dynamic disorders. But static disorder caused by structural changes is predominant in glasses. This structural disorder indicates the amount of band tails of electron density states [47]. SZLK system have shown slightly lower Urbach energies than that of BZLK system. The higher Urbach energies of BZLK glasses may be due to replacement of BaO (Ba^{2+} ionic radius is 1.35A^0) in place of SrO (Sr^{2+} ionic radius is 1.18A^0).

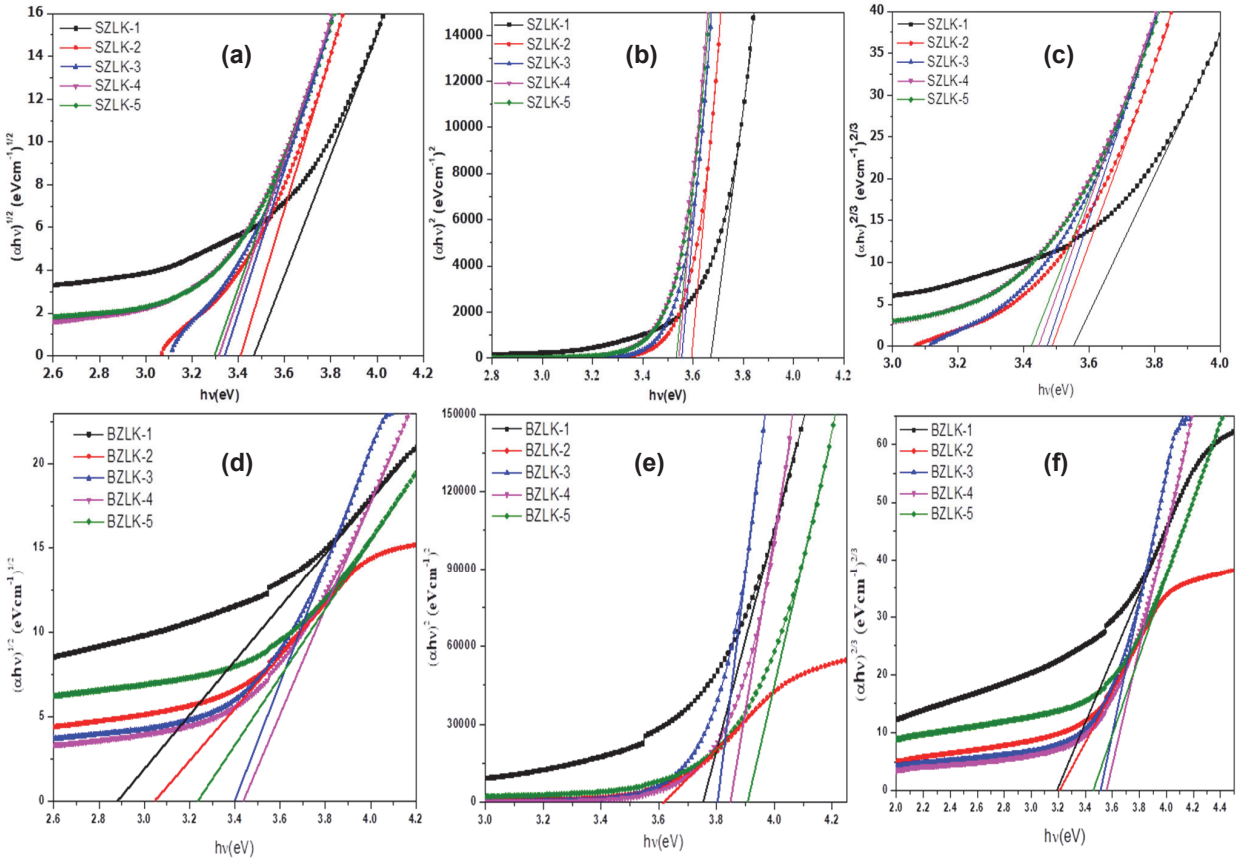

Figure 9. Tauc plots of SZLK glasses: a) indirect, b) direct allowed; c) indirect allowed and BZLK glasses: d) indirect, e) direct allowed; f) indirect allowed.

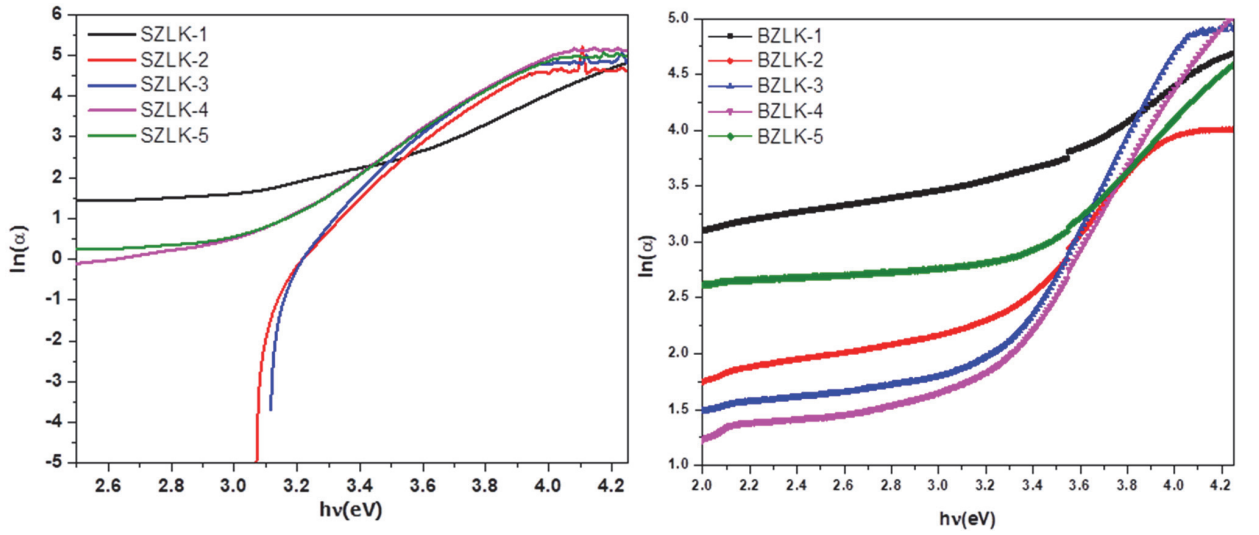

Figure 10. Estimation of Urbach energies from ln(α) versus hu plots

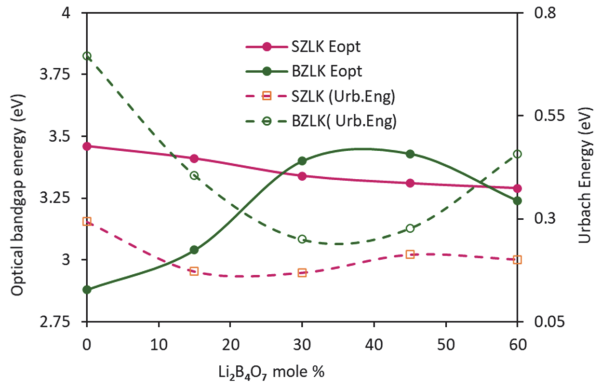

Fig.11 Variation of optical bandgap energy and Urbach energy with $Li_2B_4O_7$ mole %

4.3 Refractive Index, Electronic Polarizability and Optical Basicity

Refractive indices (*n*) of the samples are calculated by the following expression [48,49] and are given in **Table.5**

$$\frac{n^2-1}{n^2+2} = 1 - \sqrt{\frac{E_{opt}}{20}} \quad (14)$$

The refractive indices values of SZLK glass systems and BZLK glass systems are almost in the same range. The variation in '*n*' with $Li_2B_4O_7$ content in the glass has shown a small inflection at 30 mol% of $Li_2B_4O_7$ (= 30 mol% $K_2B_4O_7$). The change in the refractive indices values can be attributed to changes in density and dielectric constant in each glass system. The average molar refraction (R_m-cm^3/mol) is evaluated using the Lorentz- Lorentz equation [44].

$$R_m = \frac{n^2-1}{n^2+2} * V_m \quad (15)$$

The molar electronic polarizability (α_m in 0^{-24} cm^3) is evaluated using R_m values in Clausius-Mosotti relation.

$$\alpha_m = \left(\frac{3}{4\Pi N_A}\right) * R_m \quad (16)$$

The electronic polarizability of oxide ions $\alpha_o^{2-}(E_{opt})$ are estimated using Dimitrov and Sakka relation [49].

$$\alpha_o^{2-}(E_{opt}) = \left[\left(\frac{V_m}{2.52}\right)\left(1 - \sqrt{\frac{E_{opt}}{20}}\right) - \Sigma\alpha_i\right](N_{o^{2-}})^{-1} \quad (17)$$

Here, $[(n^2-1)/(n^2+2)]$ is reflection loss, V_m is molar volume, N_A is the Avogadro's number, Σαi is molar cation polarizability and N_O^{2-} is the number of oxide ions in the chemical formula. The molar Polarizability of cation (α_i) values are taken from the literature [44, 49]. The variation of refractive index and molar refraction (R_m) with x mol% are shown in **Fig.12**.

The metallization criterion *M* is used to determine metallic or insulating of glasses. The metallization parameter *M* values of glass samples vary around 0.40 indicating semiconducting type and perhaps have good ionic conductivity due to Li^+ ion or K^+ ion migration in the glass network.

The electronic polarizability (α_m), molar refraction (R_m), Metallization Criterion (*M*), refractive index (*n*) and dielectric constant (ε) of the glass samples are provided in **Table.5**. The non-linearity shown by the glass samples in some of the parameters might have caused by the progressive augmentation of Li atoms in place of K atoms. This substitution of atoms might caused more stress due to the insertion of Li atoms. The overall stress faced by K and Li atoms should

have reached optimum when the content of Li atoms equals the content of K atoms [50]. The observed non-linear variation and inflection with substitution of $Li_2B_4O_7$ progressively cause significant structural changes and is attributed to mixed alkali effect.

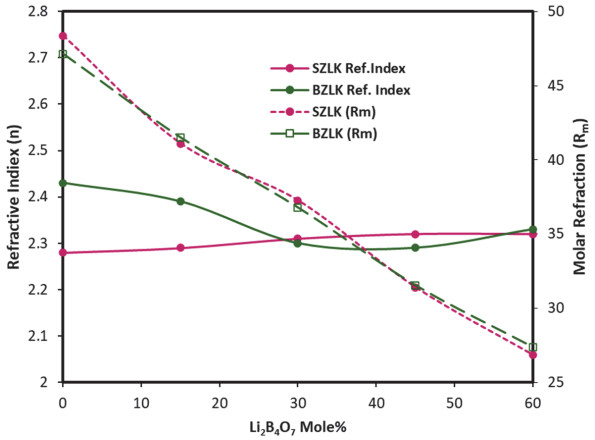

Figure 12. Variation of refractive index and molar refraction with $Li_2B_4O_7$ mole %.

4.4 Optical Basicity and oxygen packing density (OPD)

The electron donating capability of oxygen atom is measured by acidity or basicity of an oxide glass. The basicity of a glass is generally expressed optical basicity [12, 51]. In the calculation of theoretical optical basicity (Λ_{th}), optical basicity values of individual oxides are taken from the literature [38]. Optical basicity and oxide ion polarizability (α_o^{2-}) are related by [52]

$$\Lambda_{Exp} = 1.67\left(1 - \frac{1}{\alpha_0^{2-}}\right) \quad (18)$$

The values of Λ_{exp} and Λ_{th} are mentioned **Table.5.** The values of two glass systems SZLK and BZLK declined with an increase of $Li_2B_4O_7$ mol%. The minimal changes of optical basicity values are accompanied by the slight modification of charge on the oxygen ions in network.

The oxygen packing density (OPD) of the samples is arrived from density (ρ) values by the formula:

$$OPD = \frac{\rho}{M} xO_n \quad (19)$$

Here *M* represents molecular weight of the glass in mole fraction and O_n is the number of oxygen atoms per formula unit. The values of OPD are provided in **Table.5.** The higher OPD values with $Li_2B_4O_7$ content in the glass signifies greater compactness of the glass systems.

Table .5 *density (ρ), molar volume (V_m), Urbach energy (ΔE), Molar refraction (R_m), oxygen packing density (OPD), theoretical basicity (Λ_{th}), experimental basicity (Λ_{exp}), electronic polarizability (α_m), electronic polarizability of oxide ion (α_O^{2-}), metallization criteria (M), $\Sigma\alpha_{cation,}$ refractive index (n), dielectric constant (ε), reflection loss (R), No. of oxygen atoms (N_O^{2-}), Optical energy band gaps (E_{opt}), No of BO_3 and BO_4 units of the glasses*

Parameters	Glass code									
	SZLK1	SZLK2	SZLK3	SZLK4	SZLK5	BZLK1	BZLK2	BZLK3	BZLK4	BZLK5
ρ (g/cm^3)	2.63	2.82	2.81	2.96	3.02	2.99	3.05	2.98	3.08	3.18
V_m (cm^3/mol)	82.80	70.01	63.01	52.95	45.17	75.95	67.95	62.58	53.86	45.82
ΔE (eV)	0.293	0.172	0.169	0.213	0.201	0.696	0.406	0.250	0.277	0.450
R_m (cm^{-3})	48.36	41.10	37.26	31.41	26.85	47.13	41.5	36.78	31.55	27.38
OPD (mole/l)	55.55	65.70	73.00	86.87	101.83	60.56	67.69	73.50	85.41	100.38
Λ_{th}	1.767	1.707	1.647	1.587	1.527	1.772	1.712	1.652	1.592	1.532
Λ_{exp}	1.255	1.182	1.134	1.037	0.935	1.242	1.184	1.124	1.036	0.944
α_m (x10^{-24} cm^3)	19.17	16.29	14.77	12.45	10.64	18.68	16.43	14.58	12.51	10.85
α_O^{2-}	4.03	3.43	3.12	2.64	2.27	3.90	3.44	3.06	2.64	2.30
M	0.415	0.412	0.408	0.406	0.405	0.379	0.389	0.412	0.414	0.402
$\Sigma\alpha_{cation}$	0.666	0.550	0.434	0.318	0.202	0.739	0.623	0.507	0.391	0.275
n	2.28	2.29	2.31	2.32	2.32	2.43	2.39	2.30	2.29	2.33
ε	5.21	5.26	5.34	5.37	5.39	5.90	5.69	5.28	5.24	5.45
R	0.152	0.154	0.156	0.157	0.158	0.173	0.167	0.154	0.153	0.160
N_O^{2-}	4.6	4.6	4.6	4.6	4.6	4.6	4.6	4.6	4.6	4.6
E_{opt} (eV)										
indirect allowed	3.46	3.41	3.34	3.31	3.29	2.88	3.04	3.4	3.43	3.24
Direct allowed	3.67	3.59	3.55	3.54	3.53	3.75	3.62	3.8	3.84	3.90
Direct forbidden	3.55	3.48	3.47	3.44	3.42	3.19	3.21	3.51	3.55	3.46
Indirect forbidden	3.24	3.21	3.19	3.17	3.15	2.16	2.66	3.16	3.12	2.71
N_3 (BO_3)	0.488	0.495	0.487	0.502	0.503	0.492	0.491	0.495	0.482	0.497
N_4 (BO_4)	0.512	0.505	0.513	0.498	0.497	0.508	0.509	0.505	0.518	0.503

5. CONCLUSIONS

Alkaline earth oxide containg two alkali tetraborate glass systems namely 10RO-30ZnO-x$Li_2B_4O_7$-(60-x)$K_2B_4O_7$ (R=SrO, BaO) were preared by conventional melt queching process. The peakless x-ray difraction patterns indicated non-crystalline characterisitcs of prepared glass samples. The following inferences were drawn from the present studies:

- The structural landscaping investigations by FTIR and Raman spectroscopy unveiled that the glass samples contain various structural groups like diborate, triborate, tetra and penta borate units of BO_3 and BO_4 groups. The basic tetra borate structure was raptured by the alkaline earth oxide and ZnO. Eventually the structural landscape of SZLK and BZLK glasses consisted interconnected random glass network of various BO_3 and BO_4 units.
- The existence of Sr^{2+} and Ba^{2+} ions and Zn-O stretching and bending vibrations of O-Zn-O of ZnO_4 tetrahedra were confirmed by Raman and FTIR studies.
- The observed structural changes were attributed to mixed alkali effect (MAE).
- From EPR and optical absoprtion spectroscopic analysis of glasses doped with copper, $g_{||}$ and $A_{||}$ values changed non-linearly with composition. There was a possibility of competition between Cu^{2+} ions and oxide cations Sr^{2+}, Ba^{2+} and Zn^{2+} to attract oxygen ions nearest to them. Hence non-linear changes in spin-Hamiltonians, bonding coefficients and normalised covalencies were attributed to structural fluctuations.
- As one alkali tetra borate ($K_2B_4O_7$) was replaced by another ($Li_2B_4O_7$) in the glass matrix, The overall stress faced by K and Li atoms should have reached optimum when the content of Li atoms equals the content of K atoms and thereby various properties of glass samples had exhibited inflections. The structural changes were random and conversion of BO_3 triangles into BO_4 tetrahedra are not considerable since N_3 and N_4 values remained almost constant.
- The physical and optical properties such as density, molar volume, optical energy band gap, Urbach energy, molar refractivity, optical basicity and oxygen packing density have shown an inflections. The two alkalis had competition between them to take up various structural locations in the glass network causing the so called mixed alkali effect (MAE). These glasses are good media for ion conduction and hence suitable as ion conductors to preapre solid state batteries.

ACKNOWLEDGEMENTS

The authors thank Sophisticated Analytical Instrument Facility (SAIF-IIT-Mumbai) for the recording of Electron Spin Resonance spectra, Central Sophisticated Instrumentation Facility (CSIF)-BITS-Goa for x-ray diffractograms and Raman spectra recording, Head, Department of Physics, Osmania University, Hyderabad for providing FTIR spectroscopy, and Principal, Vasavi College of Engineering (Autonomous), Hyderabad for providing sample preapration facilities.

REFERENCES

1. H. Aljawhara H. Almuqrin, Ashok Kumar, J.F.M. Jecong, Nuha Al-Harbi, E. Hannachi, M.I. Sayyed (2021) Li_2O-K_2O-B_2O_3-PbO glass system: Optical and gamma-ray shielding investigations, Optik, 247,167792. doi: 10.1016/j.ijleo.2021.167792.
2. V. Arunkumar, V. Banagar, M. Prashant Kumar, S. Sunanda, N. Nagaraja (2021) Mixed Alkali Effect in Structural and Electrical Conductivity Properties of V_2O_5-, K_2O- and Na_2O-Containing Borate Glasses, J. of Elec Mater., 50, 4924–4932. doi: 10.1007/s11664-021-09000-9.
3. M. Fernandes Graça, M. Valente (2017) Ferroelectric glass-ceramics, Matter. Res.Sci. Bulletin, 42(3) 213-219. doi: 10.1557/mrs.2017.32.
4. K. Pradeesh, C.J. Oton, V.K. Agotiya, M. Raghavendra, G. Vijaya Prakash (2008) Optical properties of Er3+ doped alkali chlorophosphate glasses for optical amplifiers, Optical Materials,31(2),155-160. doi: 10.1016/j.optmat.2008.02.007.
5. V.T. Adamiv, Y.V. Burak, D.J. Wooten, J. McClory, J. Petrosky, I. Ketsman, Jie Xiao, Y.B. Losovyj, Peter A. Dowben (2010) The Electronic Structure and Secondary Pyroelectric Properties of Lithium Tetraborate, Materials (Basel), 3(9), 4550–4579. doi: 10.3390/ma3094550.
6. A. Murali, R.P.S. Chakradhar, J. Lakshmana Rao (2005) Allowed and forbidden hyperfine structure of Mn^{2+} ions in sodium tetraborate glasses-an EPR and optical study, Physica B Condensed Matter, 358 (1-4), 19–26. doi: 10.1016/j.physb.2004.12.021.
7. N.M. Bobkova, S.A. Khot'ko (2005) Zinc Oxide in Borate Glass-Forming Systems, Glass and Ceramics, 62, 167–170. doi: 10.1007/s10717-005-0064-7.
8. V.C. Veeranna Gowda, R.V. Anvekar (2004) Elastic properties and spectroscopic studies of lithium lead borate glasses, Ionics, 10, 103-108. doi: 10.1007/BF02410315.
9. Y.B. Saddeek, K.A. Aly, Safaa A Bashier (2010) Optical study of lead borosilicate glasses, Physica B Con-

densed Matter, 405(10), 2407-2412. doi: 10.1016/j.physb.2010.02.055.

10. Y.B. Saddeek, E. R. Shaaban, El Sayed Moustafa, Hesham, M. Moustafa (2008) Spectroscopic properties, electronic polarizability and optical basicity of Bi_2O_3–Li_2O–B_2O_3 glasses, Physica B: Condensed Matter, 403 (13-16), 2399-2407. doi: 10.1016/j.physb.2007.12.027.
11. F. Lodesani, M. C. Menziani, H. Hijiya, Y. Takato, S. Urata, A. Pedone (2020) Structural origins of the Mixed Alkali Effect in Alkali Aluminosilicate Glasses: Molecular Dynamics Study and its Assessment, Scientific Reports, 10, 2906. doi:10.1038/s41598-020-59875-7.
12. H. Othman, H. Elkholy, M. R. Cicconi, D. Palles, D. de Ligny, E. I. Kaisos, D. Möncke (2020) Spectroscopic study of the role of alkaline earth oxides in mixed borate glasses-site basicity, polarizability and glass structure, J. Non-Cryst. Solids, 533, 119892. doi: 10.1016/j.jnoncrysol.2020.119892.
13. A. Atila, Y. Ouldhnini, S. Ouaskit, A. Hasnaoui (2002) Atomistic insights into the mixed-alkali effect in phosphor-silicate glasses, Phys. Rev. B, 105, 134101. doi: 10.1103/PhysRevB.105.134101.
14. M. Kavgacı, H. Yaykaşlı, H. Eskalen, E. K. Perişanoğlu, S. Kalecik, R. Yılmaz, H. Tunç (2024) An experimental analysis of the effects of SrO on the mechanical, structural, optical, and nuclear radiation shielding properties of barium borate glasses, Optical Materials, 149, 114975. doi: 10.1016/j.optmat.2024.114975.
15. S. Biradar, A. Dinkar, Manjunatha, A.S. Bennal, G.B. Devidas, B.T. Hareesh, M.K. Siri, K.N. Nandan, M.I. Sayyed, H. Es-soufi, M.N. Chandrashekara (2024) Comprehensive investigation of borate-based glasses doped with BaO: An assessment of physical, structural, thermal, optical, and radiation shielding properties, Optical Materials, 150, 115176. doi: 10.1016/j.optmat.2024.115176.
16. T. Liu, Bin Duan, Y. Q. Li, C. Chun Ding (2023) The role of different alkaline earth oxide composition in copper borate glasses: Structure and optical properties, J. Non-Cryst. Solids., 604,122134. doi: 10.1016/j.jnoncrysol.2023.122134.
17. T. Walia, K. Singh (2021) Mixed alkaline earth modifiers effect on thermal, optical and structural properties of SrO-BaO-SiO_2-B_2O_3-ZrO_2 glass sealants, J. of Non-Cryst. Solids., 564, 120812. doi: 10.1016/j.jnoncrysol.2021.120812.
18. A. Shearer, M. Molinaro, M. Montazerian, J. J. Sly, M. Miola, F. Baino, J. C. Mauro (2024) The unexplored role of alkali and alkaline earth elements (ALAEs) on the structure, processing, and biological effects of bioactive glasses, Biomaterials Science, 12, 2521-2560. doi: 10.1039/D3BM01338C.
19. A. A El-Daly, M.A.Abdo, H.A. Bakr, M.S. Sadeq (2022) Structure, stability and optical parameters of cobalt zinc borate glasses, Ceramics International, 47(22), 31470-31475. doi: 10.1016/j.ceramint.2021.08.024.
20. L. Heuser, M. Nofz (2022) Alkali and alkaline earth zinc and lead borate glasses: Structure and properties, J. Non-Cryst. Solids: X, 15,100109. doi: 10.1016/j.nocx.2022.100109.
21. S.G. Motke, S.P. Yawale, S.S. Yawale S (2002), Infrared spectra of zinc doped lead borate glasses, Bull. Mater. Sci., 25(1), 75–78. doi: 10.1007/BF02704599.
22. A.A. Ali, Y.S. Rammah, M.H. Shaaban (2019) The influence of TiO_2 on structural, physical and optical properties of B_2O_3–TeO_2–Na_2O–CaO glasses, J. Non-Cryst. Solids, 514(15), 52-59. doi: 10.1016/j.jnoncrysol.2019.03.030.
23. Ao Li, M. Wang, Mei Li, Z. Liu, Y. Hu, X. Zhang (2018) The effect of mixed alkali on structural changes and ionic migration characteristics in zinc borate glasses, Materials Chemistry and Physics, 217, 519-526, doi: 10.1016/j.matchemphys.2018.07.013.
24. R. A. Elsad, M. Ahmed, Abdel-Aziz, Emad M. Ahmed, Y.S. Rammah, F.I. El-Agawany, M.S. Shams (2021) FTIR, ultrasonic and dielectric characteristics of neodymium (III)/ erbium (III) lead-borate glasses: experimental studies, J. Matter. Res. and Tech.,13,1363-1373. doi: 10.1016/j.jmrt.2021.05.029.
25. B. Tirumala Rao, B. R. Venkateswara Rao, K. Venkata Rao, S. Ravi Kumar, Ch. Rajyalakshmi, G.V.L. Kanth, G. Rama Swamy, S. Cole (2022) XRD, EPR and FT-IR Studies of Zinc Aluminium Lithium Borate (ZALB) Glasses Doped with Cu^{2+} Ions, Phys. Chem. Res., 10(4),455-460. doi:10.22036/pcr.2022.315242.1987.
26. G. Padmaja, P. Kistaiah (2009) Infrared and Raman Spectroscopic Studies on Alkali Borate Glasses: Evidence of Mixed Alkali Effect, J. of Phys. Chem A, 113(11), 2397–2404. doi: 10.1021/jp809318e.
27. C. Gautam, A. K. Yadav, A. K. Singh (2012) A Review on Infrared Spectroscopy of Borate Glasses with Effects of Different Additives, International Scholarly Research Notices 2012, 1-17. doi:10.5402/2012/428497.
28. W.L Fong, Kh. A. Bashar, S.O.Baki, M.H.M. Zaid, B.T. Goh, M.A. Mahdi (2021) Thermal, structural and optical properties of Bi_2O_3-Na_2O-TiO_2-ZnO-TeO_2 glass system, J. Non-Cryst. Solids, 555, 120621. doi: 10.1016/j.jnoncrysol.2020.120621.
29. E. M Anghel, M. Zaharescu, S. Zuca, E. Pavlatou (1999) Structure and phase diagram of the Na-$_2B_4O_7$-Na_3AlF_6 system, J. Mater. Sci., 34, 3923–3929, doi: 0.1023/A:1004635109184.
30. D. Maniu, I. Ardelean, T. Iliescu, S. Cıˆnta, V. Nagel, W. Kiefer (1999) Raman spectroscopic investigations on oxide glass system (1-x) $[3B_2O_3{\cdot}K_2O]{\cdot}xTiO_2$, J. Molecular Structure 480–481,657–659. doi:10.1016/S0022-2860(98)00831-X.
31. T. Yano, N. Kunimine, S. Shibata, M. Yamane (2003) Structural investigation of sodium borate glasses and melts by Raman spectroscopy: I Quantitative evaluation of structural units, J. Non-Cryst. Solids, 321(3), 137-146. doi: 10.1016/S0022-3093(03)00158-3.
32. B. Topper, D. Möncke, R. E. Youngman, C. Valvi, E. I. Kamitsos, C. P.E. Varsamis (2023) Zinc borate

glasses: properties, structure and modelling of the composition-dependence of borate speciation, Phys. Chem. Chem. Phys., 25,5967-5988. doi: 10.1039/D2CP05517A.

33. Z. Shan, Y. Zhang, S. Liu, H. Tao, Y. Z.Yue (2020) Mixed-alkali effect on hardness and indentation-loading behavior of a borate glass system, J. Non-Cryst. Solids, 548,120314. Doi: 10.1016/j.jnoncrysol.2020.120314.
34. M. Subhadra, P. Kistaiah (2012) Infrared and Raman spectroscopic studies of alkali bismuth borate glasses: Evidence of mixed alkali effect, Vibrational Spectroscopy, 62, 23-27. doi: 10.1016/j.vibspec.2012.07.001.
35. Y.D. Yiannopoulos, G.D. Chryssikos, E. I. Kamitsos (2001) Structure and properties of alkaline earth borate glasses, Phys. Chem. Glasses, 42(3), 164–72.
36. H.M.H. Zakaly, S.A.M. Issa, H.O. Tekin, Ali Badawi, H.A. Saudi, A.M.A. Henaish, Y.S. Rammah (2022) An experimental evaluation of CdO/PbO-B_2O_3 glasses containing neodymium oxide: Structure, electrical conductivity and gamma-ray resistance, Materials Research Bulletin, 151,111828. doi: 10.1016/j.materresbull.2022.111828.
37. A. A. Osipov, L. M. Osipova (2013) Raman scattering study of barium borate glasses and melts, J. Phys. and Chem. of Solids, 74(7), 971-978. doi: 10.1016/j.jpcs.2013.02.014.
38. J. L. Rao, G. Sivaramaiah, N.O. Gopal (2004) EPR and optical absorption spectral studies of Cu^{2+} ions doped in alkali lead tetraborate glasses. Physica B Condensed Matter, 349(1-4), 206-213, doi:10.1016/j.physb.2004.03.089.
39. B. Srinivas, B. Ashok, P. Naresh, Abdul Hameed, M. Narasimha Chary, Md. Shareefuddin (2022) Effect of SrO and TeO_2 on the physical and spectral properties of strontium tellurite boro-titanate glasses doped with Cu^{2+} ions, J. Non-Cryst. Solids, 575, 21218. doi: 10.1016/j.jnoncrysol.2021.121218.
40. S. Vedavyas, K.C. Sekhar, S. Ahammed, G. Ramadevudu, M. Narasimha Chary, Md. Shareefuddin (2021) Physical and structural studies of cadmium lead boro-tellurite glasses doped with Cu^{2+} ions. J Mater Sci: Mater Electron 32, 3083–3091. doi: 10.1007/s10854-020-05058-z.
41. C.Maalegoundla, K.C. Sekhar, A. Hameed, B. Srinivas, Md. Shareefuddin (2022) Physical and spectroscopic studies of CaF_2-Al_2O_3-Bi_2O_3-B_2O_3-CuO glasses, J Aust Ceram Soc., 58, 1137–1146. doi:10.1007/s41779-022-00737-y.
42. M. D. Ingram (2001) Amorphous Materials: Mixed Alkali Effect, Encyclopedia of Materials: Science and Technology, 220–223. doi :10.1016/b0-08-043152-6/00047-4.
43. J. Bhemarajam, P. Syam Prasad, M. Mohan Babu, M. Özcan, M. Prasad (2021) Investigations on Structural and Optical Properties of Various Modifier Oxides (MO = ZnO, CdO, BaO, and PbO) Containing Bismuth Borate Lithium Glasses. J. Compos. Sci. 5(12), 308. doi: 10.3390/jcs5120308.
44. S. L. Srinivasa Rao, G. Ramadevudu, Md. Shareefuddin, Abdul Hameed, M. Narasimha Chary, M. Lakshmipathi Rao (2012) Optical properties of alkaline earth borate glasses, Int. J Engg, Sci. and Tech, 4(4), 25-35. doi: 10.4314/ijest.v4i4.3.
45. G. Srinivas, B. Ramesh, J. Siva Kumar, Md. Shareefuddin, M.N.Chary, R. Sayanna (2016) Mixed alkali effect in the physical and optical properties of xK_2O-(25-x) Na_2O-12.5MgO-12.5BaO-50B_2O_3 glasses, J. Taibah University for Science, 10(3), 442-449. doi: 10.1016/j.jtusci.2015.09.002.
46. R.P. S. Chakradhar, G. Sivaramaiah, J. L. Rao, N.O. Gopal (2005) EPR and optical investigations of manganese ions in alkali lead tetraborate glasses, Spectro Chimica Acta Part A: Molecular and Biomolecular Spectroscopy,62(4–5), 761-768. doi: 10.1016/j.saa.2005.02.045.
47. I.A Weinstein, A.F Zatsepin, V.S Kortov (2001) Effects of structural disorder and Urbach's rule in binary lead silicate glasses, J. Non-Cryst. Solids, 279(1),77-87. doi:10.1016/S0022-3093(00)00396-3.
48. B. Eraiah (2006) Optical properties of samarium doped zinc–tellurite glasses, Bull. Mater. Sci., 29(4), 375–378. doi:10.1007/BF02704138.
49. V. Dimitrov, S. Sakka (1996) Electronic oxide polarizability and optical basicity of simple oxides-I, J. Appl. Phy, 79(3),1736-40. doi:10.1063/1.360962.
50. Y. Yu, J. C. Mauro, M. Bauchy (2017) Stretched Exponential Relaxation of Glasses: Origin of the Mixed Alkali Effect, American Ceramic Society Bulletin 96(4),34-36. doi:10.48550/arXiv.1801.01969.
51. V. Dimitrov, T. Komatsu (1999), Electronic polarizability, optical basicity and non-linear optical properties of oxide glasses, J. Non-Cryst. Solids, 249(2–3),160-179. doi:10.1016/S0022-
52. H. Doweidar, Y. B. Saddeek (2009) FTIR and ultrasonic investigations on modified bismuth borate glasses, J. Non-Cryst. Solids,355(6),348-354. doi: 10.1016/j.jnoncrysol.2008.12.008.

IZVOD

ISTRAŽIVANJE STRUKTURA I FIZIČKIH SVOJSTAVA RO-ZNO-$LI_2B_4O_7$-$K_2B_4O_7$ (RO= SRO I BAO) STAKLA

Uzorci stakla 10RO-30ZnO-k$Li_2B_4O_7$-(60-k) $K_2B_4O_7$ (RO=SrO i BaO) sa alkalnim tetra boratima u rasponu od 0 do 60 mol% proizvedeni su tradicionalnim postupkom gašenja. Široki rendgenski difrakcijski obrasci bez vrha utvrdili su amorfnu osobinu uzoraka stakla. FTIR i Raman spektroskopska analiza je pokazala postojanje strukturnih grupa BO_3 i BO_4 zajedno sa drugim jedinicama borata. Na stopu konverzije $BO_3 \Leftrightarrow BO_4$ nije mnogo uticala varijacija jednog od alkalnih tetraborata. EPR spektri stakla dopiranih bakrom potvrdili su osnovno stanje Cu^{2+} jona kao 2B1g. Utvrđeno je da fizička i optička svojstva, odnosno gustina, molarna zapremina, indeks prelamanja, molarna refrakcija, optički pojas i Urbahova energija zavise od sastava. Pregibi uočeni u gustini i drugim optičkim svojstvima oko jednakih mol% alkalnih oksida u sistemu stakla pripisani su strukturnim modifikacijama i mešovitom alkalnom efektu. Ovi rezultati su razotkrili strukturne varijacije uzrokovane konkurentnošću između dva različita alkalna i alkalna oksida u zauzimanju geometrijskih pozicija mreže boratnog stakla.

Ključne reči: *mešani alkalni efekat (MAE), zemnoalkalna stakla, optički pojas, elektronska paramagnetna rezonanca, FTIR i Ramanova spektroskopija*

Naučni rad
Rad primljen: 11.04.2024.
Rad korigovan: 31.05.2024.
Rad prihvaćen: 9.06.2024.

The ORCID Ids of all the authors are as follows:
Sarap Krishnaprasad: https://orcid.org/0009-0008-2979-1316
Mohammed Shareefuddin: https://orcid.org/0000-0003-3747-1917
Siddey Laxmi Srinivasa Rao: https://orcid.org/0009-0006-5635-1557
Gokarakonda Ramadevudu: https://orcid.org/0000-0002-9931-1778